Assessment of Satellite and Reanalysis Precipitation Products for Rainfall-Runoff Modelling in a Mountainous Basin[†]

Hamed Hafizi [1,2] and Ali Arda Sorman [1]*

[1] Department of Civil Engineering, Eskisehir Technical University, Eskisehir, Turkey; hamedha-fizi@eskisehir.edu.tr, asorman@eskisehir.edu.tr
[2] Department of Hydraulics and Hydraulic Structures, Faculty of Environmental and Water Resources Engineering, Kabul Polytechnic University, Kabul, Afghanistan; hamedhafizi@kpu.edu.af
*   Correspondence: asorman@eskisehir.edu.tr
†   Presented at the 4th International Electronic Conference on Atmospheric Sciences, 16–31 July 2021; Available online: https://ecas2021.sciforum.net/.

Abstract: Precipitation measurement over complex topography and high elevated regions has always been a great challenge in the recent decades. On the other side, satellite-based and numerical weather prediction model outputs can be an alternative to fill this gap. Hence, the goal of this study is to evaluate the spatio-temporal stability and hydrologic utility of four precipitation products (TMPA-3B42v7, IMERGHHFv06, ERA5 and PERSIANN) over a mountainous basin (Karasu basin) located in the eastern part of Turkey. Moreover, Kling Gupta Efficiency (KGE) including its correlation, bias and variability ratio components are used for direct comparison of precipitation products (PPs) with observed gauge data and Hansen-Kuiper (HK) score is utilized to assess the detectability strength of PPs for different precipitation events. In the same way, the hydrologic utility of PPs is tested by exploiting a conceptual rainfall-runoff model under Kling Gupta Efficiency (KGE) and Nash-Sutcliffe Efficiency (NSE) metrics. Generally, all PPs show low performance for the direct comparison with observed data while their performance considerably increases for streamflow simulation. TMPA-3B42v7 has a high reproducibility in streamflow (KGE=0.84) followed by IMERGHHFv06 (KGE=0.76), ERA5 (KGE=0.75) and PERSIANN (KGE=0.70) for the entire period (2015-2019) in this study.

Keywords: Precipitation products; Validation; Rainfall-Runoff modeling; Mountainous basin; Turkey

1. Introduction

High spatial and temporal resolution precipitation estimates are essential for dealing with problems related to water resources management, flood forecasting, agricultural forecasts and natural hazards [1,2]. Moreover, utilizing hydrologic models for rainfall-runoff simulation in a basin always need accurate precipitation estimates which are limited for most regions [3]. Precipitation estimation by rain gauge network is one of the well-known methods and provide the opportunity of direct physical measurement of precipitation with high accuracy above the ground level [4,5]. However, rain gauges are limited over time and space and usually the network is denser in low lying areas. The high-land regions typically referred as having complex topography suffer from gauge scarcity that cause detrimental effects in rainfall-runoff simulations over mountainous basins [6-9].

In the recent years, precipitation derived from satellites using Passive Microwave (PMW) and Infrared (IR) sensor information and numerical weather prediction model outputs can be an alternative in poorly gauged regions around the world. Hence, Satellite and Reanalysis Precipitation Products (PPs) have been implemented for numerous hy-

drometeorological studies, such as rainfall-runoff simulation [10], natural hazard [11], climate change [12] as well as renewable energy [13].

Moreover, a number of Precipitation Products (PPs) with different spatial and temporal resolution from various sources have been developed, such as Tropical Rainfall Measuring Mission (TRMM) Multi-satellite Precipitation Analysis (TMPA) 3B42v7 [14], Integrated Multi-satellitE Retrievals for the Global Precipitation Measurement (GPM) Half Hourly (IMERGHH) final run v06 [15], European Centre for Medium Range Weather Forecasts (ECMWF) reanalysis fifth generation (ERA5) [16] and Precipitation Estimation from Remotely Sensed Information using Artificial Neural Networks (PERSIANN) [17].

Furthermore, the application of hydrologic models has received considerable attention for solving the real-world problems related to water resources management and development and the hydrologic models' structures varies from simple to very sophisticated considering the level of information used in the model for a particular problem [18-20].

The consistency of different PP has been caried out by several authors in regional and global scales around the world [21-23]. However, the reliability of PPs over a specific area is not applicable for another region and an individual assessment is needed to address the stability of PPs. While different studies have been caried out to address the reliability of some PPs over Turkey [24-26], previous studies either considered only direct comparison excluding the hydrologic utility or modeling has been taken into account in a coarse time step such as monthly. In this work, we consider both direct PP comparison including seasonal variability and utilize PPs in hydrologic modeling in a daily time step.

The aim of this study is to evaluate both meteorological and hydrological stability of four PPs (TMPA-3B42v7, IMERGHHFv06, ERA5 and PERSIANN) considering the seasonal variability of precipitation in daily time step for 5 water years from October 2014 to September 2019.

The structure of this paper is as follow: Section 1 present a comprehensive introduction to PPs. Section 2 of this study give information of materials and methods. Section 3 present the results and detailed discussions and finally, conclusions are conveyed in Section 4.

2. Materials and Methods

2.1. Study area

With a drainage area of around 10250 km², Karasu river originates the headwaters of the largest basin (Euphrates) in Turkey situated within 38⁰ 58' E to 41⁰ 39' E and 39⁰ 23'
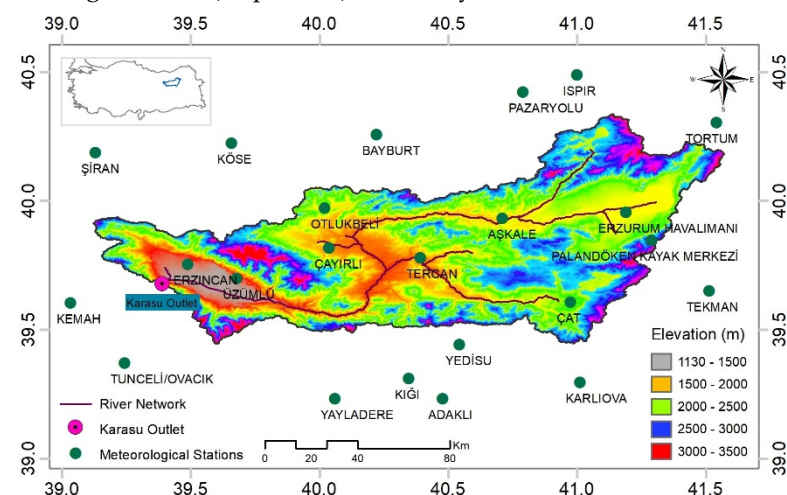
Figure 1. Geographical location, Basin Elevation (m), meteorological stations and hydrological station located at the study area.

N to 40º 25' N. The basin elevation varies from 1130 m to 3500 m and the outlet is controlled by Kemah Boğazı (E21A019) stream gaging station (Figure 1).

2.2. Data

In the study, daily precipitation and temperature data from 23 meteorological stations are provided by General Directorate of Meteorology (GDM) and streamflow data at the basin outlet (E21A019) is obtained from General Directorate of Hydraulic Works (GDHW) for 5 water years (October 2014 to September 2019). Moreover, daily precipitation from four PPs, TRMM Multi-satellite Precipitation Analysis (TMPA) 3B42v7, Integrated Multi-satellitE Retrievals for GPM (IMERG) Half Hourly final runv06, European Centre for Medium Range Weather Forecasts (ECMWF) reanalysis fifth generation (ERA5) and Precipitation Estimation from Remotely Sensed Information using Artificial Neural Networks (PERSIANN) are acquired from different sources for validation. The properties of selected GPDs are summarized in Table 1.

Table 1. Properties of selected PPs, Abbreviations in the data source column; G, gauge; S, satellite; R; Reanalysis.

Name	Data source(s)	Spatial resolution	Spatial coverage	Temporal resolution	Reference
TMPA-3B42v7	G, S	0.25º	50º N/S	3-hourly	[14]
IMERGHHFv06	G, S	0.10º	60º N/S	30 min	[15]
ERA5	R	0.25º	50º N/S	Hourly	[16]
PERSIANN	S	0.25º	60º N/S	Hourly	[17]

2.3. Methodology

For the direct comparison of PPs with observed precipitation, Kling Gupta Efficiency (KGE) [27,28] which is a combination of correlation, bias and variability ratio is utilized . In the same way, Hansen-Kuiper (HK) score is used to measure the detectability strength of PPs for five different precipitation categories based on World Meteorological Organization [29] and modified by Zambran Bigiarini [30]. The five precipitation thresholds considered are: no-precipitation (less than 1 mm/day), light precipitation (1-5 mm/day), moderate precipitation (5-20 mm/day), heavy precipitation (20-40 mm/day) and violent precipitation (more than 40 mm/day). Moreover, Nash–Sutcliffe Efficiency (NSE) and KGE are selected to evaluate the hydrologic utility of PPs for streamflow simulation. Two scenarios are considered in this case; firstly, the model parameters are calibrated using observed precipitation by ground stations and then PPs are replaced and tested individually (scheme-1). Secondly, the model parameters are calibrated and validated for each PP independently (scheme-2). Table 2 shows the properties of selected evaluation metrics whereby the optimal value is unity for each of them.

For the hydrologic modeling part, TUW model, a conceptual hydrologic model developed by the Technical University of Vienna and built based-on the similar structure of HBV model is utilized operating at daily time scale. TUW model has 15 parameters and is able to simulate runoff, snow and soil moisture using inputs from daily accumulated precipitation, daily average temperature and daily potential evapotranspiration. Moreover, for model parameter calibration observed streamflow is demanded by the model. Information on 15 model parameters are summarized in Table 3.

Table 2. Properties of performance indices for evaluation of PPs

Performance indicator	Mathematical statement	Explanation
Kling Gupta Efficiency and its components	$KGE=1-[(R-1)^2+(\beta-1)^2+(VR-1)^2]^{0.5}$ $R=\dfrac{1}{n}\sum_{1}^{n}(o_n-\mu_0)(s_n-\mu_s)/(\delta_o\times\delta_s),$ $\beta=\dfrac{\mu_s}{\mu_o},\quad VR=(\delta_s\times\mu_o)/(\mu_s\times\delta_o)$	R is *Pearson correlation coefficient*, β *(Bias)* is the ratio of estimated and observed mean, *VR (Variability Ratio)* is the ratio of estimated and observed coefficients of variation, μ and δ are the distribution mean and standard deviation where *s* and *o* indicate estimated and observed.
Hansen-Kuiper	$HK=\dfrac{(H\times CN)-(F\times M)}{(H+M)\,(F+CN)}$	*M (Miss)*; when the observed precipitation is not detected. *F (False)*; when the precipitation is detected but not observed, *H (Hit)*; when the observed precipitation is correctly detected, *CN (Correct Negative)*; a no precipitation event is detected.
Nash–Sutcliffe Efficiency	$NSE=1-\dfrac{\sum_{i=1}^{n}(Q_i^{sim}-Q_i^{ob})^2}{\sum_{i=1}^{n}(Q_i^{ob}-\overline{Q_i^{ob}})^2}$	n is the sample size of the observed or calculated streamflow. Q_i^{ob} and Q_i^{sim} present the observed and simulated streamflow, $\overline{Q_i^{ob}}$ present the mean observed streamflow.

3. Result and discussion

3.1. Mean daily precipitation

Figure 2 shows the mean daily precipitation from observed and four PPs including their bias over the study area for the entire period (2014-2019) and four seasons. Overall, the region receives 1.5 mm/day precipitation for the entire period where this amount increases to 2.2 mm/day during the spring and reduces to 0.7 mm/day in the summer. Precipitation during autumn (1.1 mm/day) is less when compared to winter (1.8 mm/day).
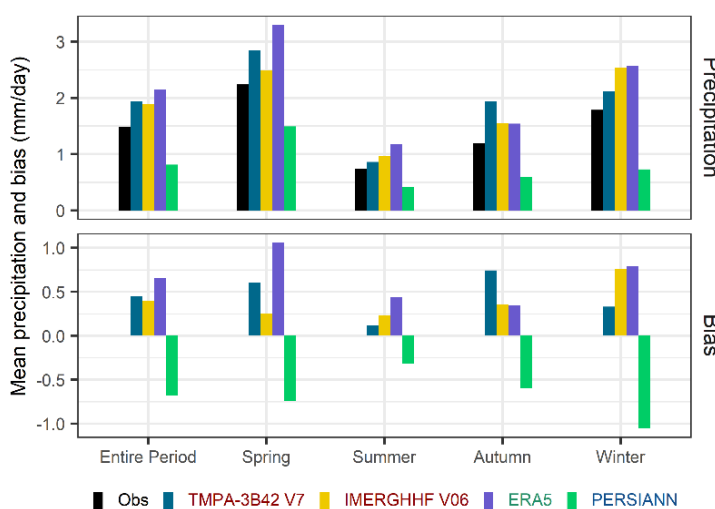
Figure 2. Mean daily precipitation and its bias compared to observed over the study region for the entire period and four seasons.

Furthermore, among all PPs, PERSIANN always underestimate precipitation while the others show an overestimation of mean daily precipitation, ERA5 giving the highest overestimate (bias; 1.1 mm/day) during spring season. Both IMERGHHFv06 and ERA5

show close mean daily precipitation during autumn and winter seasons while TMPA-3B42v7 display more precipitation (1.9 mm/day) during autumn season and present the lowest bias (0.12 mm/day) in the summer, comparatively.

3.2. Quantitative and Categorial performance of PPs

Figure 3 indicates the median of Kling Gupta Efficiency (KGE) including its three components for the entire period and four seasons. All PPs perform weak for daily precipitation in Karasu basin where the highest performance is given by ERA5 (median KGE; 0.27) during the autumn season. Moreover, among gauge corrected PPs, TMPA-3B42v7 show the highest bias (1.61) over the study area for the entire period where IMERGHHFv06 significantly overestimate bias (median of bias; 2.14) during winter. Furthermore, PERSIANN always underestimate bias and overestimate variability ratio for the entire period and four seasons.
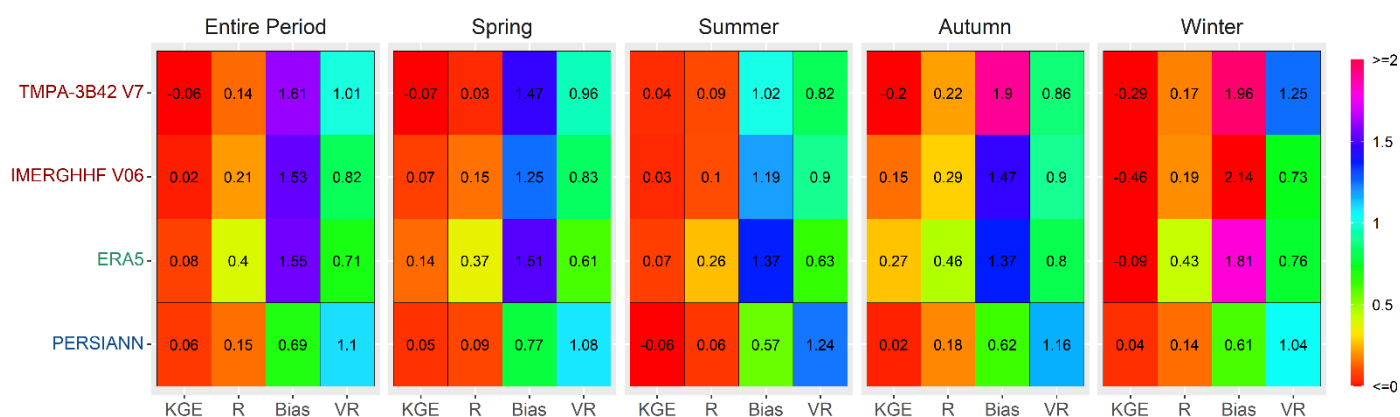

Figure 3. PPs reliability at the regional scale under Kling Gupta Efficiency (KGE) and its components for daily precipitation considering the entire period and four seasons. Y-axis color presents: satellite [blue], gauge and satellite [red], Reanalysis [green].

Figure 4 presents the detectability strength of selected PPs for five precipitation intensities which is evaluated by Hansen-Kuiper (HK) score considering entire period and four seasons. Generally, PPs show better detectability for low intensity daily precipitation and their detectability strength decrease by increasing precipitation intensities. Among PPs, ERA5 show high detectability for precipitation less than 1 mm/day for the entire period and this amount increases to 0.47 during autumn season. Moreover, ERA5 present better detectability for moderate precipitation overall. All PPs show higher detectability for moderate precipitation compared to light precipitation. IMERGHHFv6 show higher detectability compared to TMPA-3B42v7 for precipitation less than 1 mm
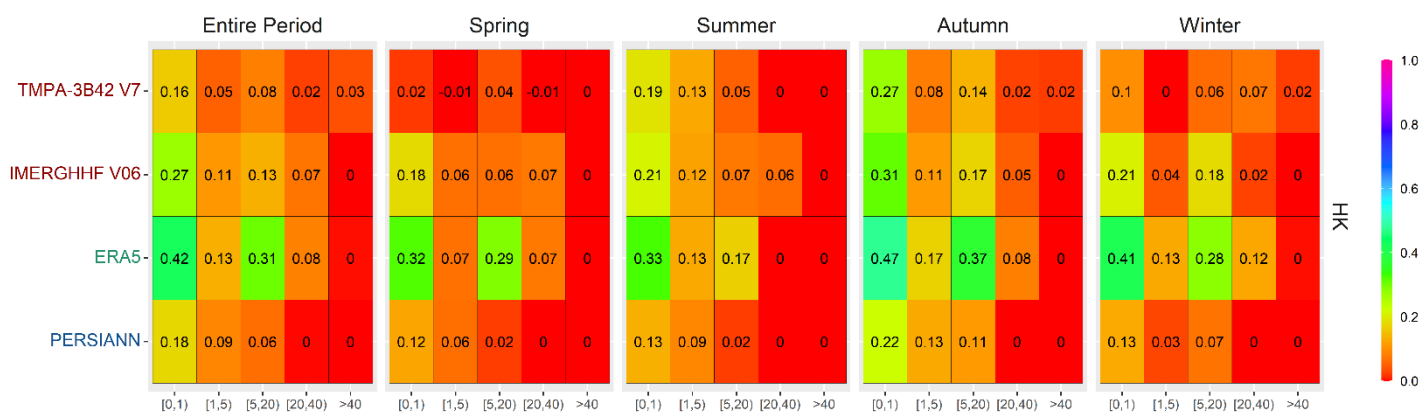

Figure 4. PPs detection ability in reproducing daily precipitation intensities expressed in the form of Hansen-Kuiper (HK) score considering the entire period and four seasons. Y-axis color presents: satellite [blue], gauge and satellite [red], Reanalysis [green].

/day. PERSIANN performed weak for capturing different precipitation events, comparatively.

3.3. Hydrologic utility of PPs

Figure 5 displays the observed and simulated hydrographs in two schemes including gauge precipitation and PPs for Karasu basin. Daily streamflows are reproduced by the TUW model for 5 water years classified into two parts: model calibration (October 2014 to
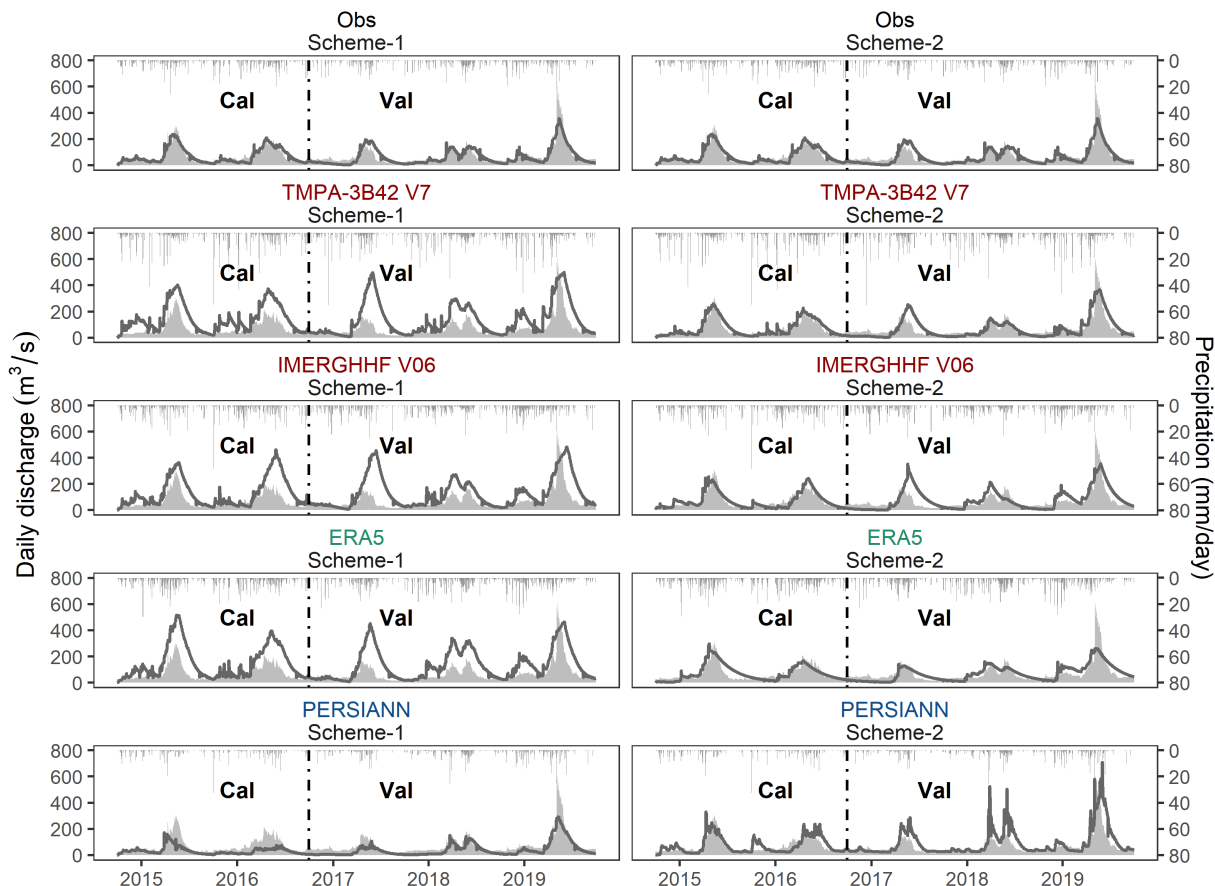
Figure 6. Hydrographs of observed and simulated daily discharge based on observed precipitation and four PPs for calibration (October 2014 to September 2016) and validation (October 2016 to September 2019) period in two schemes.

September 2016) and validation (October 2016 to September 2019). Figure 6 maps the performance of PPs for streamflow simulation at the Karasu basin outlet. The model displays a high performance using gauge observations both in the calibration and vali-
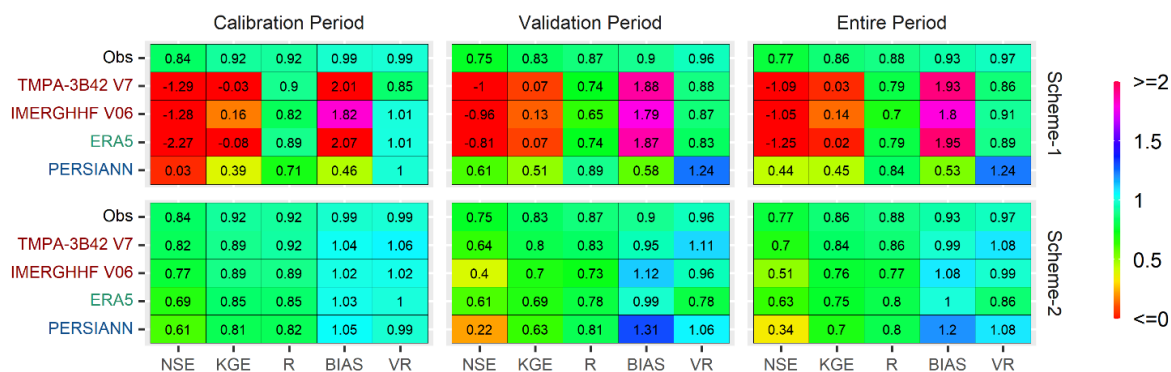
Figure 5. Performance of daily streamflow for observed precipitation and selected PPs.

dation periods. On the other hand, PPs do not show the same success in scheme-1 although having high correlation ratios and high bias. Only PERSIANN indicates an unusual behavior with a low calibration and high validation simulation. Furthermore, when the model parameters are calibrated by each PP individually, all PPs show high reproducibility of streamflow for calibration period and acceptable ranges for validation. For scheme-2, PERSIANN again performed unexpectedly exhibiting the lowest results of all PPs. Table 3 summarizes TUW model parameter ranges and calibration results for observed and PPs.

Table 3. Model parameter range and optimum values for observed and PPs. Number of the column indicates; 0, parameter range; 1, Obs; 2,TMPA-3B42v7; 3, IMERGHHFv06; 4, ERA5; 5, PERSIANN

Parameter and units	0	1	2	3	4	5
Snow correction factor - SCF (-)	0.9 - 1.5	1.44	1.12	1.03	0.91	1.46
Degree-day factor - DDF (mm/°C /day)	0.0 - 5.0	0.36	0.3	0.51	0.36	0.33
Temperature threshold above which precipitation is rain- Tr (°C)	1.0 - 3.0	2.51	1.74	1.43	2.92	2.99
Temperature threshold below which precipitation is snow Ts (°C)	- 3.0 – 1.0	-1.01	-0.01	-0.1	-2.13	1
Temperature threshold above which melt starts - Tm (°C)	- 2.0 – 2.0	-0.5	-1.86	0.87	-0.92	1.87
Parameter related to the limit for potential evaporation - Lpart (-)	0.0 - 1.0	0.88	0.6	0.36	0.82	0.69
Field capacity - FC (mm)	0.0 - 600	132.2	317.8	45.3	115.3	591.5
Non-linear parameter for runoff production - Beta (-)	0.0 - 20	0.97	1.82	5.52	14.75	0.05
Constant percolation rate - K0 (mm/day)	0.0 - 2.0	0.69	1.09	0.73	1.2	1.34
Storage coefficient for very fast response - K1 (day)	2.0– 30	26.39	23.12	20.06	27	27.08
Storage coefficient for fast response -K2 (day)	30 - 250	36.1	38.3	50.9	78.5	245.5
Storage coefficient for slow response - lsuz (day)	1.0 - 100	51.8	87.9	57.5	46.4	98.4
Threshold storage state - cperc (mm)	0.0- 8.0	6.44	5.03	6.97	6.79	0.39
Maximum base at low flows - bmax (day)	0.0 - 30	14.23	13.65	7.78	7.45	15.4
Free scaling parameter - croute (day2/mm)	0.0 - 50	17.81	27.37	24.35	29.37	5.32

4. Conclusions

In this study, the reliability of four PPs (TMPA-3B42v7, IMERGHHFv06, ERA5 and PERSIANN) is tested by direct comparison of PPs with observed precipitation obtained from 23 ground stations. Moreover, the hydrologic utility of each PP on runoff is evaluated for 5 water years (October 2014 to September 2019) at the mountainous Karasu basin. Several performance metrics (KGE, HK and NSE) are considered for the meteorological and hydrological evaluation. The major conclusions are summarized as follows:

- All PPs show high detectability for low intensity precipitation where their detectability strength decreases for high intensity precipitation for the considered entire period and four seasons. Furthermore, ERA5 shows high detectability in almost all precipitation events compared to other PPs.
- In the direct comparison, all PP performances (median of KGE varies from -0.06 of TMPA-3B42v7 to 0.08 of ERA5) are low for daily precipitation during the entire period. Although PP correlations (R) are higher, high/low bias and variability ratios cause detrimental effects.
- PPs show a better reproducibility for streamflow when evaluated against direct precipitation comparison with gauge data. Moreover, PPs are able to estimate streamflow with high accuracy if model parameters are calibrated by PPs individually. TMPA-3B42v7 shows the highest performance for streamflow simulation both in calibration (NSE; 0.82) and validation (NSE; 0.64) periods in scheme-2, followed by IMERGHHFv6 and ERA5. PERSIANN shows variable

performance in both schemes for calibration/validation and has the lowest performance of all PP in scheme-2.

Future work will include more PPs for direct precipitation comparison as well as hydrologic simulations.

References

1.   Zhang, Y.; Sun, A.; Sun, H.; Gui, D.; Xue, J.; Liao, W.; Yan, D.; Zhao, N.; Zeng, X. Error adjustment of TMPA satellite precipitation estimates and assessment of their hydrological utility in the middle and upper Yangtze River Basin, China. *Atmospheric research* **2019**, *216*, 52-64, doi:10.1016/j.atmosres.2018.09.021.

2.   Indu, J.; Kumar, D.N. Copula-based modeling of TMI brightness temperature with rainfall type. *IEEE transactions on geoscience and remote sensing* **2013**, *52*, 4832-4845, doi:10.1109/TGRS.2013.2285225.

3.   Talchabhadel, R.; Aryal, A.; Kawaike, K.; Yamanoi, K.; Nakagawa, H.; Bhatta, B.; Karki, S.; Thapa, B.R. Evaluation of precipitation elasticity using precipitation data from ground and satellite-based estimates and watershed modeling in Western Nepal. *Journal of Hydrology: Regional Studies* **2021**, *33*, 100768, doi:10.1016/j.ejrh.2020.100768.

4.   Berg, P.; Norin, L.; Olsson, J. Creation of a high resolution precipitation data set by merging gridded gauge data and radar observations for Sweden. *Journal of Hydrology* **2016**, *541*, 6-13, doi:10.1016/j.jhydrol.2015.11.031.

5.   Shi, H.; Chen, J.; Li, T.; Wang, G. A new method for estimation of spatially distributed rainfall through merging satellite observations, raingauge records, and terrain digital elevation model data. *Journal of Hydro-environment Research* **2017**, doi:10.1016/j.jher.2017.10.006.

6.   Jeffrey, S.J.; Carter, J.O.; Moodie, K.B.; Beswick, A.R. Using spatial interpolation to construct a comprehensive archive of Australian climate data. *Environmental Modelling & Software* **2001**, *16*, 309-330, doi:10.1016/S1364-8152(01)00008-1.

7.   Li, M.; Shao, Q. An improved statistical approach to merge satellite rainfall estimates and raingauge data. *Journal of Hydrology* **2010**, *385*, 51-64, doi:10.1016/j.jhydrol.2010.01.023.

8.   Gourley, J.J.; Vieux, B.E. A method for identifying sources of model uncertainty in rainfall-runoff simulations. *Journal of Hydrology* **2006**, *327*, 68-80, doi:10.1016/j.jhydrol.2005.11.036.

9.   Xue, X.; Hong, Y.; Limaye, A.S.; Gourley, J.J.; Huffman, G.J.; Khan, S.I.; Dorji, C.; Chen, S. Statistical and hydrological evaluation of TRMM-based Multi-satellite Precipitation Analysis over the Wangchu Basin of Bhutan: Are the latest satellite precipitation products 3B42V7 ready for use in ungauged basins? *Journal of Hydrology* **2013**, *499*, 91-99, doi:10.1016/j.jhydrol.2013.06.042.

10.   Le, M.-H.; Lakshmi, V.; Bolten, J.; Du Bui, D. Adequacy of satellite-derived precipitation estimate for hydrological modeling in Vietnam Basins. *Journal of Hydrology* **2020**, *586*, 124820, doi:10.1016/j.jhydrol.2020.124820.

11.   Li, X.; Chen, S.; Liang, Z.; Huang, C.; Li, Z.; Hu, B. Performance Assessment of GSMaP and GPM IMERG Products during Typhoon Mangkhut. *Atmosphere* **2021**, *12*, 134, doi:10.3390/atmos12020134.

12.   Aznarez, C.; Jimeno-Sáez, P.; López-Ballesteros, A.; Pacheco, J.P.; Senent-Aparicio, J. Analysing the Impact of Climate Change on Hydrological Ecosystem Services in Laguna del Sauce (Uruguay) Using the SWAT Model and Remote Sensing Data. *Remote Sensing* **2021**, *13*, 2014, doi:10.1596/30472.

13.   Doddy Clarke, E.; Griffin, S.; McDermott, F.; Monteiro Correia, J.; Sweeney, C. Which Reanalysis Dataset Should We Use for Renewable Energy Analysis in Ireland? *Atmosphere* **2021**, *12*, 624, doi:10.3390/atmos12050624.

14.   Huffman, G.J.; Adler, R.F.; Bolvin, D.T.; Nelkin, E.J. The TRMM multi-satellite precipitation analysis (TMPA). In *Satellite rainfall applications for surface hydrology*; Springer: 2010; pp. 3-22.

15.   Huffman, G.J.; Bolvin, D.T.; Braithwaite, D.; Hsu, K.-L.; Joyce, R.J.; Kidd, C.; Nelkin, E.J.; Sorooshian, S.; Stocker, E.F.; Tan, J. Integrated Multi-satellite Retrievals for the Global Precipitation Measurement (GPM) Mission (IMERG). In *Satellite Precipitation Measurement*; Springer: 2020; pp. 343-353.

16. Hersbach, H.; Dee, D. ERA5 reanalysis is in production, ECMWF Newsletter, Vol. 147. *Reading, United Kingdom: ECMWF www. ecmwf. int/sites/default/files/elibrary/2016/16299newsletterno147spring2016. pdf* **2016**.

17. Hsu, K.l.; Gupta, H.V.; Gao, X.; Sorooshian, S. Estimation of physical variables from multichannel remotely sensed imagery using a neural network: Application to rainfall estimation. *Water Resources Research* **1999**, *35*, 1605-1618, doi:10.1029/1999WR900032.

18. Nguyen, H.H.; Recknagel, F.; Meyer, W.; Frizenschaf, J.; Ying, H.; Gibbs, M.S. Comparison of the alternative models SOURCE and SWAT for predicting catchment streamflow, sediment and nutrient loads under the effect of land use changes. *Science of The Total Environment* **2019**, *662*, 254-265, doi:10.1016/j.scitotenv.2019.01.286.

19. Singh, V.P. Hydrologic modeling: progress and future directions. *Geoscience Letters* **2018**, *5*, 1-18, doi:10.1186/s40562-018-0113-z.

20. Krysanova, V.; Srinivasan, R. Assessment of climate and land use change impacts with SWAT. **2015**, doi:10.1007/s10113-014-0742-5.

21. Ghorbanpour, A.K.; Hessels, T.; Moghim, S.; Afshar, A. Comparison and assessment of spatial downscaling methods for enhancing the accuracy of satellite-based precipitation over Lake Urmia Basin. *Journal of Hydrology* **2021**, *596*, 126055, doi:10.1016/j.jhydrol.2021.126055.

22. Zhao, N. An Efficient Downscaling Scheme for High-Resolution Precipitation Estimates over a High Mountainous Watershed. *Remote Sensing* **2021**, *13*, 234, doi:10.3390/rs13020234.

23. Wang, W.; Lin, H.; Chen, N.; Chen, Z. Evaluation of multi-source precipitation products over the Yangtze River Basin. *Atmospheric Research* **2021**, *249*, 105287.

24. Aksu, H.; Akgül, M.A. Performance evaluation of CHIRPS satellite precipitation estimates over Turkey. *Theoretical and Applied Climatology* **2020**, *142*, 71-84, doi:10.1007/s00704-020-03301-5.

25. Amjad, M.; Yilmaz, M.T.; Yucel, I.; Yilmaz, K.K. Performance evaluation of satellite-and model-based precipitation products over varying climate and complex topography. *Journal of Hydrology* **2020**, *584*, 124707, doi:10.1016/j.jhydrol.2020.124707.

26. Irvem, A.; Ozbuldu, M. Evaluation of Satellite and Reanalysis Precipitation Products Using GIS for All Basins in Turkey. *Advances in Meteorology* **2019**, *2019*, doi:10.1155/2019/4820136.

27. Gupta, H.V.; Kling, H.; Yilmaz, K.K.; Martinez, G.F. Decomposition of the mean squared error and NSE performance criteria: Implications for improving hydrological modelling. *Journal of hydrology* **2009**, *377*, 80-91, doi:10.1016/j.jhydrol.2009.08.003.

28. Kling, H.; Fuchs, M.; Paulin, M. Runoff conditions in the upper Danube basin under an ensemble of climate change scenarios. *Journal of Hydrology* **2012**, *424*, 264-277, doi:10.1016/j.jhydrol.2012.01.011.

29. WMO. Guide to Hydrological Practices. Volume I. Hydrology–From Measurement to Hydrological Information. **2008**, doi:10.1080/02626667.2011.546602.

30. Zambrano-Bigiarini, M.; Nauditt, A.; Birkel, C.; Verbist, K.; Ribbe, L. Temporal and spatial evaluation of satellite-based rainfall estimates across the complex topographical and climatic gradients of Chile. *Hydrology and Earth System Sciences* **2017**, *21*, 1295, doi:10.5194/hess-21-1295-2017.